miR378a-3p in serum extracellular vesicles is associated with pancreatic beta-cell mass in diabetic states

Yokoi, Aisha ; Asahara, Shun-ichiro ; Inoue, Hiroyuki ; Goto, Ayano ; Seike, Masako ; Kido, Nozomi ; Suzuki, Hirotaka ; Kanno, Ayumi ;…

(Citation)
Biochemical and Biophysical Research Communications,750:151367

(Issue Date)
2025-03

(Resource Type)
journal article

(Version)
Version of Record

Biochemical and Biophysical Research Communications 750 (2025) 151367

Contents lists available at ScienceDirect

Biochemical and Biophysical Research Communications

journal homepage: www.elsevier.com/locate/ybbrc

miR378a-3p in serum extracellular vesicles is associated with pancreatic beta-cell mass in diabetic states

Aisha Yokoi [a], Shun-ichiro Asahara [a,*], Hiroyuki Inoue [b], Ayano Goto [b], Masako Seike [a], Nozomi Kido [a], Hirotaka Suzuki [a], Ayumi Kanno [a], Maki Kimura-Koyanagi [a], Kenichi Uto [c], Jun Saegusa [d], Yoshiaki Kido [b], Wataru Ogawa [a]

[a] Division of Diabetes and Endocrinology, Department of Internal Medicine, Kobe University Graduate School of Medicine, 7-5-1 Kusunoki-cho, Chuo-ku, Kobe, Hyogo, 650-0017, Japan
[b] Division of Medical Chemistry, Department of Metabolism and Diseases, Kobe University Graduate School of Health Sciences, 7-10-2 Tomogaoka, Suma-ku, Kobe, Hyogo, 654-0142, Japan
[c] Department of Clinical Laboratory, Kobe University Hospital, 7-5-2 Kusunoki-cho, Chuo-ku, Kobe, Hyogo, 650-0017, Japan
[d] Department of Rheumatology and Clinical Immunology, Kobe University Graduate School of Medicine, 7-5-1 Kusunoki-cho, Chuo-ku, Kobe, Hyogo, 650-0017, Japan

ARTICLE INFO

Keywords:
Extracellular vesicles
β-cell
miR378a-3p
Diabetes

ABSTRACT

The condition in which the insulin secretory ability of pancreatic β-cells decreases in diabetes is extremely important, but there are currently no biomarkers that reflect pancreatic β-cell failure. Therefore, we conducted a search for biomarkers, using pancreatic β-cell-specific 3-Phosphoinositide-dependent protein kinase 1 (PDK1) knockout mice, which develop severe hyperglycemia due to a decrease in pancreatic β-cell mass without insulin resistance. The analysis was performed in young mice when metabolic abnormalities were not yet apparent. Comprehensive analysis of microRNAs contained in extracellular vesicles in the blood of these mice revealed that miR378a-3p levels were significantly lower in PDK1 knockout mice than in control mice. Furthermore, in other mouse models of diabetes, namely, db/db mice and streptozotocin-induced diabetic mice, there was an increase and decrease in miR378a-3p expression, respectively, in line with the number of β-cells. These results suggest that miR378a-3p contained in serum extracellular vesicles is a biomarker that reflects pancreatic β-cell mass before the onset of diabetes. It is hoped that miR378a-3p can be utilized to realize earlier diagnosis and treatment of diabetes.

1. Introduction

Diabetes is one of the leading causes of death and disability worldwide, affecting people of all ages, both sexes, and all countries. It is estimated that more than 500 million people worldwide had diabetes, with a global age-standardized total prevalence of diabetes of 6.1 % (5.8%–6.5 %) in 2021. The majority of cases are diagnosed as type 2 diabetes, accounting for 96.0 % (95.1%–96.8 %) of all cases in 2021 [1].

The pathogenesis of type 2 diabetes comprises two factors: insulin resistance, which reduces the efficacy of insulin, and a decrease in insulin secretion from pancreatic β-cells [2]. Insulin resistance refers to a condition in which insulin does not function normally in target organs such as the liver, skeletal muscle, central nervous system, and adipose tissue, even though the concentration of insulin is increased in the blood. Meanwhile, a decrease in insulin secretion is caused by a reduction in the number of pancreatic β-cells, which are the only cells that secrete insulin, or by abnormalities in the insulin secretion mechanism [3]. It has been reported for some time that a decrease in the number of pancreatic β-cells begins well before the onset of diabetes, and that hyperglycemia becomes apparent when β-cell mass has decreased by approximately 80 % [4]. In Asian populations in particular, a compensatory increase in pancreatic β-cell volume is also unlikely to occur,

* Corresponding author. Division of Diabetes and Endocrinology, Department of Internal Medicine, Kobe University Graduate School of Medicine, 7-5-1 Kusunoki-cho, Chuo-ku, Kobe, Hyogo, 650-0017, Japan

E-mail addresses: hirany@med.kobe-u.ac.jp (A. Yokoi), asahara@med.kobe-u.ac.jp (S.-i. Asahara), h.inoue310@gmail.com (H. Inoue), 0604ayn@gmail.com (A. Goto), koto0125@med.kobe-u.ac.jp (M. Seike), oono3104@med.kobe-u.ac.jp (N. Kido), shirotak@med.kobe-u.ac.jp (H. Suzuki), akanno@med.kobe-u.ac.jp (A. Kanno), koyanagi@med.kobe-u.ac.jp (M. Kimura-Koyanagi), kuto@med.kobe-u.ac.jp (K. Uto), jsaegusa@med.kobe-u.ac.jp (J. Saegusa), kido@med.kobe-u.ac.jp (Y. Kido), ogawa@med.kobe-u.ac.jp (W. Ogawa).

https://doi.org/10.1016/j.bbrc.2025.151367
Received 14 January 2025; Received in revised form 15 January 2025; Accepted 19 January 2025
Available online 21 January 2025

which is considered a major pathogenic mechanism of type 2 diabetes [5]. Although there is a strong correlation between the onset of diabetes and pancreatic β-cells, there are presently no biomarkers that reflect pancreatic β-cell failure. Because β-cell failure is recognized even before blood glucose levels rise and diabetes is diagnosed, there is a strong desire to establish biomarkers that can specifically evaluate β-cell failure in order to diagnose diabetes at an earlier stage.

Extracellular vesicles (EVs) are small particles with a lipid bilayer and a diameter of 30–150 nm that are secreted by most cells in the body [6]. EVs are present in various body fluids and carry lipids, proteins, DNA, microRNAs (miRNAs), messenger RNAs (mRNAs), long non-coding RNAs, and other molecules that may be protected from degradation by nucleases that are widely present in serum [7]. The miRNAs carried by EVs (EV-miRNAs) are stable in the blood and can be reliably detected even at low concentrations [8]. Therefore, the detection of specific EV-miRNAs in the blood has the potential to provide an early diagnosis [9].

We decided to identify a new biomarker for pancreatic β-cell failure, using EVs isolated from a mouse model of pancreatic β-cell failure. To perform comprehensive analysis of EV-miRNAs, we need a model mouse that stably exhibits the pathology of pancreatic β-cell failure. The commonly used streptozotocin (STZ)-induced diabetic mouse model of pancreatic β-cell failure has a very high degree of individual variation, and leptin receptor-deficient db/db mice may be affected by other factors such as hyperlipidemia and insulin resistance. Therefore, we decided to use pancreatic β-cell-specific 3-Phosphoinositide-dependent protein kinase 1 (PDK1) knockout (βPDK1KO) mice for our analysis. We previously created and analyzed βPDK1KO mice, and reported that they exhibit a marked decrease in pancreatic β-cell mass and severe hyperglycemia [10]. βPDK1KO mice do not develop insulin resistance or dyslipidemia, and they exhibit a very uniform phenotype, so we considered that they would be a useful model for searching for biomarkers of pancreatic β-cell failure.

In this study, we used this mouse model to analyze EV-miRNAs in the blood and attempted to identify miRNAs that could be used as biomarkers to reflect the burden on pancreatic β-cells before the onset of diabetes.

2. Materials and methods

2.1. Animals

We used βPDK1KO, db/db, and STZ-induced mice as diabetic model mice. βPDK1KO mice have been described previously [10]. PDK1 flox/flox mice were used as controls. Male db/db mice on a C57BL/KsJ background (CLEA Japan, Inc., Tokyo, Japan) and STZ-induced mice were fed normal chow and maintained on a 12-h light/dark cycle. STZ (350 mg/kg; Wako, Tokyo, Japan) was reconstituted in saline and administered by a single intraperitoneal injection. Control mice were injected with saline. The study protocol, which conformed to the National Institutes of Health Guide for the Care and Use of Laboratory Animals and the ARRIVE guidelines, was approved by the Animal Ethics Committee of Kobe University Graduate School of Medicine (approval no. P201103).

2.2. RNA-seq analysis

RNA isolated from each sample was used to construct sequencing libraries with a SMARTer smRNA-Seq Kit for Illumina (TaKaRa Bio, Inc., Shiga, Japan). Briefly, input RNA was polyadenylated to provide a priming sequence for an oligo-(dT) primer. cDNA synthesis was primed by the 3′ smRNA dT primer, which incorporates an adapter sequence at the 5′-end of each RNA template, and it adds non-templated nucleotides that are bound by the SMART smRNA oligo-enhanced with locked nucleic acid technology for greater sensitivity. In the template-switching step, PrimeScript RT uses the SMART smRNA oligo as a template for the addition of a second adapter sequence to the 3′-end of each first-strand cDNA molecule. In the next step, full-length Illumina adapters (including index sequences for sample multiplexing) were added during PCR amplification. The forward PCR primer binds to the sequence added by the SMART smRNA oligo, while the reverse PCR primer binds to the sequence added by the 3′ smRNA dT primer. The resulting library cDNA molecules include sequences required for clustering on an Illumina flow cell.

The libraries were validated by checking their size, purity, and concentration on an Agilent Bioanalyzer (Agilent, Santa Clara, CA). The libraries were pooled in equimolar amounts, and sequenced on a HiSeq 2500 System (Illumina, San Diego, CA) to generate 51-bp reads. Image decomposition and quality value calculation were performed using the modules of the Illumina pipeline.

2.3. RNA extraction and miRNA expression profiling

RNA was extracted from mouse EVs using a 3D-Gene RNA Extraction Reagent from Liquid Sample Kit (Toray Industries, Kamakura, Japan). Extracted total RNA was checked using a Bioanalyzer (Agilent) and labeled with a 3D-Gene miRNA Labeling Kit (Toray Industries). Half volumes of labeled RNAs were hybridized onto a 3D-Gene (Mouse) miRNA Oligo Chip (Toray Industries). The annotation and oligonucleotide sequences of the probes conformed to the miRBase miRNA database (http://microrna.sanger.ac.uk/sequences/). After stringent washes, fluorescent signals were scanned with a 3D-Gene Scanner (Toray Industries) and analyzed using 3D-Gene Extraction software (Toray Industries).

The raw data of each spot were normalized by substitution with the mean intensity of the background signal determined by all blank spots' signal intensities with 95 % confidence intervals. Measurements of spots with signal intensities greater than 2 standard deviations of the background signal intensity were considered to be valid. A relative expression level of a given miRNA was calculated by comparing the signal intensities of the valid spots throughout the microarray experiments. The normalized data were globally normalized per array, such that the median signal intensity was adjusted to 25.

2.4. EV isolation

EVs were isolated using EVSecond L70 (GL Sciences, Tokyo, Japan). EVSecond L70 was centrifuged at 12,000×*g*, 4 °C, for 15 min with 500 μL serum, and the maximum amount of sample (100–400 μL) was collected from the middle layer. The column was inverted and mixed to ensure that the internal packing material was completely homogenized, and then placed on a fraction rack. After removing the top and bottom caps of the column and draining the storage solution, 700 μL fetal bovine serum filtered through a 0.22-μm syringe filter was added to the column for blocking. Next, 1.5 mL phosphate-buffered saline (PBS) was added three times to equilibrate the column. The sample was added dropwise, and PBS was added so that the total volume with the serum sample was 1500 μL. All effluent was discarded and a collection tube was set up to collect 12 fractions of 100 μL PBS each. All manipulations were performed at room temperature and spontaneous titration.

2.5. Enzyme-linked immunosorbent assay (ELISA)

ELISA was performed as described previously [11]. The solid-phase antibody was a purified anti-mouse CD9 antibody (125 ng/well; BioLegend, San Diego, CA), detection antibody was a biotin-conjugated anti-mouse CD9 antibody (250 ng/mL; BioLegend), streptavidin-horseradish peroxidase × 1/2000 (B-1215; Vector Laboratories, Burlingame, CA), and the substrate was 1-Step Ultra TMB-ELISA Substrate Solution (34028; Thermo Fisher Scientific, Waltham, MA). The optical density ratio of the serum samples and standard control samples was then calculated to quantify serum CD9-positive EVs.

2.6. Analysis of metabolic parameters

Whole blood samples collected from the tail of mice or serum samples obtained by centrifugation of whole blood samples twice at 15,000 rpm, 4 °C, for 15 min were used to analyze serum insulin levels with an ELISA kit (Shibayagi Co., Ltd., Gunma, Japan).

2.7. miRNA extraction and quantitative real-time PCR

Serum EV-miRNAs were extracted from the EV-containing fractions, which were confirmed by western blotting, using an miRNeasy Mini Kit (Qiagen, Hilden, Germany). A TaqMan™ MicroRNA Assay and 7500 Real-Time PCR System were used to perform quantitative real-time PCR analysis. As an invariant control, the abundance of the target miRNAs was normalized to that of let-7c-5p miRNA.

2.8. Immunoblot analysis

The extracted EV solution was dissolved in 5 × sample buffer for each fraction and subjected to 15 % polyacrylamide gel electrophoresis. The fractionated proteins were transferred to a PVDF membrane for 90 min, and the PVDF membrane was then blocked with 3 % bovine serum albumin. The membrane was incubated overnight at 4 °C with anti-CD9 (System Biosciences, Palo Alto, CA) and anti-CD81 (Santa Cruz Biotechnology, Dallas, TX) primary antibodies. The membrane was then probed with horseradish peroxidase-conjugated anti-rabbit (Promega, Madison, WI) and anti-mouse (Bio-Rad Laboratories, Hercules, CA) secondary antibodies.

2.9. Statistical analysis

Quantitative data are presented as the mean ± standard error of the mean (SEM), and differences between means were assessed with Student's *t*-test (two-tailed). A *P*-value <0.05 was considered statistically significant.

3. Results

3.1. βPDK1KO mice exhibit pancreatic β-cell failure without metabolic abnormalities at 7 weeks of age

First, we measured the metabolic data of βPDK1KO mice, and found that there was no significant difference in body weight between βPDK1KO and control mice throughout the entire course of the

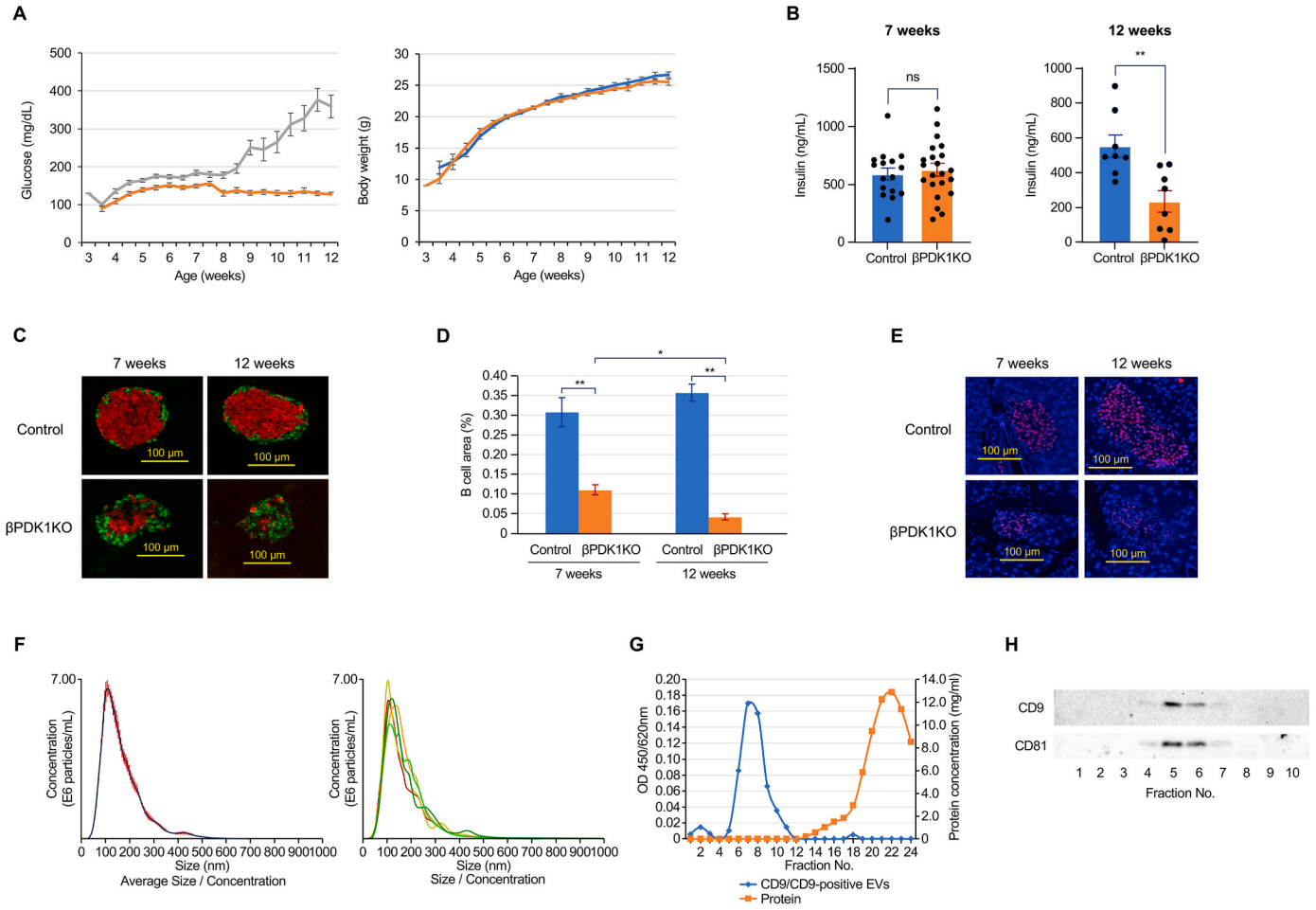

Fig. 1. Isolation of EVs from a mouse model of pancreatic β-cell failure without metabolic abnormalities. (A) Blood glucose levels in the fed state (left) and body weight (right) for βPDK1KO and control mice (PDK1 flox/flox) at various ages. (B) Serum insulin levels for 7- (left) and 12-week-old (right) βPDK1KO and control mice. (C) Immunostaining of insulin (red) and glucagon (green) in pancreatic sections from 7- and 12-week-old mice. (D) Quantification of pancreatic β-cell area in 7- (left) and 12-week-old (right) mice. (E) Immunostaining for PDX1 (red) in pancreatic islets from 7- and 12-week-old mice. (F) NanoSight analysis of averaged (left) and each (right) EV diameter and concentration isolated from βPDK1KO mice. (G) Serum EV-containing fractions were determined by EV sandwich ELISA detecting CD9-positive EVs and protein concentration by micro-BCA protein assay. (H) Immunoblot analysis of CD9 and CD81 using fractions containing serum EVs. All quantitative data are means ± SEM for (A) 10–14, (B) 16–19, or (D) 4–6 mice in each group. *$P < 0.05$; **$P < 0.01$. (For interpretation of the references to colour in this figure legend, the reader is referred to the Web version of this article.)

experiment. However, significant hyperglycemia was observed in βPDK1KO mice from 8 weeks of age (Fig. 1A). At 7 weeks of age, there was no difference between βPDK1KO and control mice in terms of serum insulin levels, but at 12 weeks of age, a significant decrease in insulin levels was observed in βPDK1KO mice (Fig. 1B). When the number of β-cells was compared, a significant decrease was observed in βPDK1KO mice from 7 weeks of age (Fig. 1C and D). When we checked pancreatic and duodenal homeobox 1 (PDX1), a typical β-cell marker, by immunostaining, we found that PDX1 expression was reduced in the islets of βPDK1KO mice from 7 weeks of age (Fig. 1E). From the above results, it was thought that pancreatic β-cell dysfunction had already occurred in βPDK1KO mice at 7 weeks of age, but there was no effect on metabolic data such as blood glucose and serum insulin levels. Therefore, to establish a biomarker for pancreatic β-cell dysfunction that excludes the effects of changes in metabolic data, we isolated serum EVs from 7-week-old mice.

When we measured serum EVs using NanoSight, which can evaluate the characteristics of nanoparticles, EVs isolated from the serum of βPDK1KO mice were 167 ± 2.5 nm in size, with 8.84×10^{10} particles/mL, which were not significantly different from the size and concentration of normal EVs (Fig. 1F). In addition, we confirmed the detection of EVs positive for CD9, which is a surface marker of EVs, using ELISA (Fig. 1G), and immunoblot analysis also confirmed the expression of CD9 and CD81, which is also a surface marker of EVs (Fig. 1H).

3.2. Integrated RNA-seq and microarray analyses of serum EVs from βPDK1KO mice reveals significantly decreased miR378a-3p expression

We extracted EV-miRNAs in the state of pancreatic β-cell failure and performed comprehensive analysis. First, we performed RNA-seq analysis using EV-miRNAs isolated from the serum of βPDK1KO mice. The miRNAs that showed significant expression changes compared to EV-miRNAs from control mice are shown in Table 1. To extract candidates from these molecules, we conducted analysis that integrated the results of RNA-seq with those of two microarray analyses. As a result of these three exhaustive analyses, we identified one EV-miRNA that was upregulated and three that were downregulated in βPDK1KO mice compared with control mice. These four miRNAs were reproducibly altered in 7-week-old βPDK1KO mice (Fig. 2A).

To compare the expression levels of these four EV-miRNAs further, we quantified their expression in serum EVs by real-time PCR. Compared with the control group, there was no difference in the expression levels of miR126a-5p, miR29b-3p, and miR122–5p in the serum EVs of βPDK1KO mice, but miR378a-3p expression was significantly decreased (Fig. 2B–E).

3.3. miR378a-3p expression in serum EVs correlates with the number of pancreatic β-cells in diabetic model mice

Previous reports have shown that pancreatic β-cell mass changes significantly in diabetic conditions [12]. Therefore, we analyzed miR378a-3p expression in serum EVs from diabetic model mice using quantitative real-time PCR. First, we analyzed miR378a-3p expression in serum EVs from db/db mice, a typical type 2 diabetic mouse model. It has been reported that the Pancreatic β-cell mass increases in db/db mice at 7 weeks of age as a compensatory response to insulin resistance [13,14], and we confirmed that the number of pancreatic β-cells in db/db mice tended to increase compared with db/m mice, as previously reported (Fig. 3A). At this point, miR378a-3p expression was significantly increased in db/db mice (Fig. 3B). In addition, STZ-induced mice, which is a model of diabetes in which hyperglycemia is induced by the specific destruction of pancreatic β-cells, there was no significant change in miR378a-3p expression at 1 day after STZ administration (Fig. 3C), but its expression was significantly decreased at 1 week after administration (Fig. 3D). These results indicate that miR378a-3p levels in serum EVs may reflect the number of pancreatic β-cells.

Table 1
RNA-seq analysis of miRNAs with increased (left) and decreased (right) expression in serum EVs of βPDK1KO mice.

miRNA	Expression levels		Ratio(KO/C)
	Control	βPDK1KO	
mmu-miR-486a-3p	300.3003	4523.181304	15.0622
mmu-miR-486b-3p	300.3003	4523.181304	15.0622
mmu-miR-221–3p	300.3003	3015.454203	10.0415
mmu-miR-455–3p	300.3003	3015.454203	10.0415
mmu-miR-423–3p	300.3003	2638.522427	8.78628
mmu-miR-744–5p	300.3003	1507.727101	5.02073
mmu-miR-328–3p	5105.105105	19977.38409	3.91322
mmu-miR-1895	300.3003	1130.795326	3.76555
mmu-miR-320–3p	300.3003	1130.795326	3.76555
mmu-miR-378a-5p	1201.201201	4146.249529	3.45175
mmu-miR-187–3p	300.3003	753.863551	2.51037
mmu-miR-28a-5p	300.3003	753.863551	2.51037
mmu-miR-28c	300.3003	753.863551	2.51037
mmu-miR-337–5p	300.3003	753.863551	2.51037
mmu-miR-466i-5p	300.3003	753.863551	2.51037
mmu-miR-5113	300.3003	753.863551	2.51037
mmu-miR-532–3p	300.3003	753.863551	2.51037
mmu-miR-6236	300.3003	753.863551	2.51037
mmu-miR-673–5p	300.3003	753.863551	2.51037
mmu-miR-99b-3p	300.3003	753.863551	2.51037
mmu-miR-532–5p	600.600601	1507.727101	2.51037
mmu-miR-486a-5p	34534.53454	74255.55974	2.15018
mmu-miR-486b-5p	34534.53454	74255.55974	2.15018
mmu-miR-106b-3p	2402.402402	4900.11308	2.03967
mmu-miR-125a-5p	15015.01502	27892.95138	1.85767
mmu-miR-99b-5p	1801.801802	3015.454203	1.67358
mmu-miR-133a-3p	3303.303303	5277.044855	1.59751
mmu-lct-7d-3p	9909.90991	15831.13457	1.59751
mmu-miR-2137	7807.807808	12438.74859	1.59751
mmu-miR-21a-5p	1201.201201	1884.658877	1.56898
mmu-miR-484	1201.201201	1884.658877	1.56898
mmu-miR-92a-3p	9909.90991	15454.20279	1.55947
mmu-miR-151–3p	3003.003003	4523.181304	1.50622
mmu-miR-126a-5p	6906.906907	9800.226159	1.4189
mmu-miR-150–5p	14114.11411	19977.38409	1.41524
mmu-miR-322–5p	3003.003003	376.931775	0.12552
mmu-miR-130b-3p	2102.102102	376.931775	0.17931
mmu-miR-22–3p	1801.801802	376.931775	0.2092
mmu-miR-29b-3p	1501.501502	376.931775	0.25104
mmu-miR-676–3p	1501.501502	376.931775	0.25104
mmu-miR-16–5p	3003.003003	753.863551	0.25104
mmu-miR-143–3p	2702.702703	753.863551	0.27893
mmu-miR-5128	3903.903904	1130.795326	0.28966
mmu-miR-130a-3p	14114.11411	4146.249529	0.29377
mmnu-miR-122–5p	8708.708709	2638.522427	0.30298
mmu-miR-133b-3p	1201.201201	3769.31775	0.3138
mmu-miR-27a-3p	1201.201201	3769.31775	0.3138
mmu-miR-99a-5p	1201.201201	3769.31775	0.3138
mmu-miR-674–5p	3603.603604	1130.795326	0.3138
mmu-miR-199a-3p	2402.402402	753.863551	0.3138
mmu-miR-199b-3p	2402.402402	753.863551	0.3138
mmu-miR-192–5p	3303.303303	1130.795326	0.34232
mmu- miR-19b-3p	3003.003003	1130.795326	0.37655
mmu-miR-146b-5p	900.900901	376.931775	0.41839
mmu-miR-181c-5p	900.900901	376.931775	0.41839
mmu-miR-185–5p	900.900901	376.931775	0.41839
mmu-miR-27b-3p	900.900901	376.931775	0.41839
mmu-miR-425–5p	900.900901	376.931775	0.41839
mmu-miR-223–3p	2702.702703	1130.795326	0.41839
mmu-miR-30a-3p	1801.801802	753.863551	0.41839
mmu-let-7g-5p	11411.41141	4900.11308	0.4294
mmu-miR-378a-3p	13213.21321	6784.771956	0.51348
mmu-miR-142a-5p	7207.207207	4146.249529	0.57529
mmu-miR126a-3p	11711.71171	7161.703732	0.6115
mmu-miR-24–3p	48948.94895	30154.54203	0.61604
mmu-miR-128–3p	6006.00601	3769.31775	06.2759
nunu-miR-139–5p	6006.00601	3769.31775	06.2759
mmu-miR-144–5p	6006.00601	3769.31775	06.2759
mmu-miR-1843b-3p	6006.00601	3769.31775	06.2759
mmu-miR-184–3p	6006.00601	3769.31775	06.2759
mmu-miR-206–3p	6006.00601	3769.31775	06.2759
mmu-miR-222–3p	600.600601	376.931775	0.62759

(*continued on next page*)

Table 1 (*continued*)

miRNA	Expression levels		Ratio(KO/C)
	Control	βPDK1KO	
mmu-miR-28a-3p	600.600601	376.931775	0.62759
mmu-miR-30d-5p	600.600601	376.931775	06.2759
mmu-miR-324–3p	600.600601	376.931775	0.62759
mmu-miR-331–3p	600.600601	376.931775	0.62759
mmu-miR-485–3p	600.600601	376.931775	0.62759
mmu-miR-181a-5p	1201.201201	753.863551	0.62759
mmu-miR-451a	15915.91592	10177.15793	0.63943
mmu-let-7i-5p	7507.507508	4900.11308	0.6527
mmu-miR-29a-3p	14714.71472	9800.226159	0.66602

Red indicates miRNAs extracted by integrated RNA-seq and microarray analyses.

4. Discussion

For many years, hemoglobin A1c and blood glucose levels have been used as diagnostic markers for diabetes. In addition, the condition and stage of the disease in daily clinical practice are evaluated by measuring and assessing blood insulin and *C*-peptide levels. However, these markers all indicate that metabolic abnormalities have already occurred, and it is thought that pancreatic β-cell failure has progressed. At present, there is no established marker for evaluating the decrease in pancreatic β-cell mass that occurs in the early stages of type 2 diabetes.

In this study, we used pancreatic β-cell-specific PDK1KO mice as a model of pancreatic β-cell failure. We thought that by isolating serum EVs from these mice at 7 weeks of age, we could search for biomarkers that would not affect metabolic data such as blood glucose and serum insulin levels. After extracting miRNAs contained in serum EVs, we conducted three comprehensive analyses using RNA-seq and microarrays. Through these integrated analyses, we identified four molecules with high reproducibility in terms of changes in their expression levels. Furthermore, when we conducted quantitative real-time PCR, miR378a-3p was significantly downregulated in serum EVs from βPDK1KO mice, as observed in the comprehensive analyses. To confirm that miR378a-3p could be used to evaluate pancreatic β-cell dysfunction in other mouse models of diabetes, we also analyzed db/db mice and STZ-induced diabetic mice. Pancreatic β-cell mass increases markedly in young db/db mice due to compensatory mechanisms against insulin resistance [13]. In fact, in 7-week-old db/db mice, when pancreatic β-cell mass had increased, there was a significant increase in miR378a-3p levels in serum EVs. In contrast, in STZ-induced diabetic mice, in which pancreatic β-cell mass decreases, there was no significant difference at 1 day after STZ administration, but a significant decrease in miR378a-3p expression was confirmed at 1 week after administration. These results show that there is a relationship between miR378a-3p levels and pancreatic β-cell mass.

There are reports that miR378a-3p expression is elevated in obese women who have undergone gastric bypass surgery [15], and that it is predominantly elevated in circulating miRNAs in pediatric obesity [16], so it is known that its expression is elevated in the blood of obese people. Because the number of β-cells increases in obese individuals [17], there may also be a correlation between miR378a-3p expression and pancreatic β-cell mass in humans.

In this study, we did not clarify the tissue origin of miR378a-3p, but previous reports have shown that its expression is upregulated in adipose tissue of high-fat diet-induced obese mice and 3T3-L1 preadipocytes [18], suggesting that it is secreted in large quantities from adipose tissue. In addition, there are reports that miR378a-3p is involved in insulin resistance and the homeostasis of oxidative metabolism in the liver [19], and there are many studies showing that miR378a-3p is an important regulator of energy and glucose homeostasis in skeletal muscle [20,21]. However, the relationship between miR378a-3p and pancreatic β-cells has not been examined, and the significance of miR378a-3p in relation to pancreatic β-cell mass and its mechanism of action are not clear, so further investigation is needed.

In recent years, there have been reports of protein disulfide isomerase as a new biomarker for diabetes, with one report suggesting that it is a biomarker for β-cell stress in type 1 diabetes [22], another report indicating that circulating glucokinase could be a biomarker for type 1 diabetes [23], and another study reporting that serotonin could be applied to the early diagnosis of diabetes [24]. However, none of these potential biomarkers have yet reached the stage of clinical application. By combining the newly identified miR378a-3p in blood EVs with these biomarkers, it is hoped that a new diagnostic method with higher

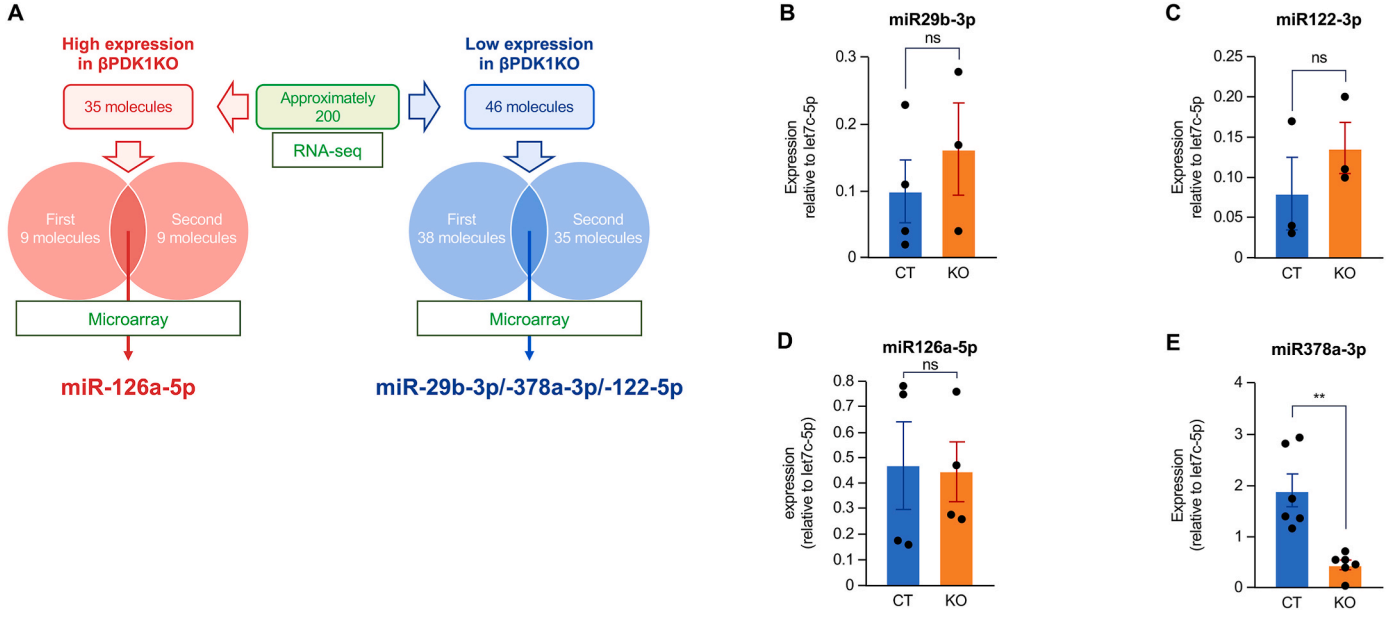

Fig. 2. Comprehensive analysis and quantitative real-time PCR shows increased miR378a-3p expression within EVs of βPDK1KO mice. (A) Diagram of integrated RNA-seq and microarray analyses for miRNA expression in serum EVs of βPDK1KO mice. (B–E) Confirmation of the expression of miR29b-3p (B), miR122–5p (C), miR126a-5p (D), and miR378a-3p (E) by quantitative real-time PCR in serum EVs of βPDK1KO mice. All quantitative data are means ± SEM for (B) 3–4, (C) 3, (D) 4, or (E) 5 mice in each group. $^{*}P < 0.05$; $^{**}P < 0.01$.

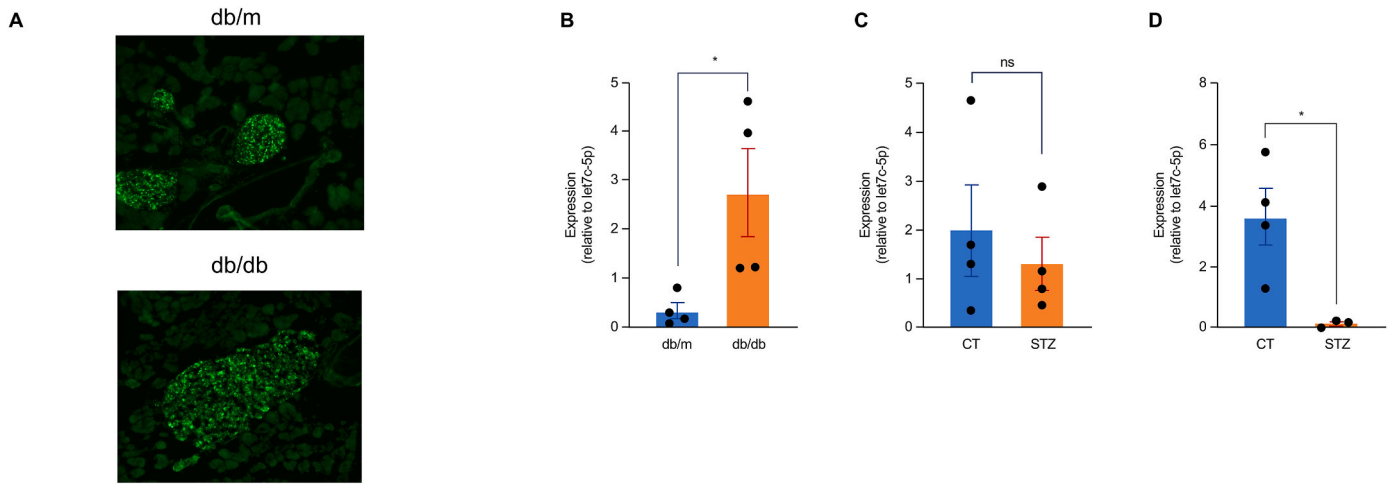

Fig. 3. Correlation between pancreatic β-cell mass and miR378a-3p expression in EVs is also observed in db/db and STZ-induced diabetic mice. (A) Immunostaining of insulin (green) in pancreatic sections from 7-week-old db/m and db/db mice. (B) Quantitative real-time PCR analysis of miR378a-3p expression in serum EVs of db/m and db/db mice. (C) Quantitative real-time PCR analysis of miR378a-3p expression in serum EVs of STZ-induced diabetic mice at 1 day after STZ administration. (D) Quantitative real-time PCR analysis of miR378a-3p expression in serum EVs of STZ-induced diabetic mice at 1 week after STZ administration. All quantitative data are means ± SEM for (B) 4, (C) 4, or (D) 3–4 mice in each group. $*P < 0.05$; $**P < 0.01$. (For interpretation of the references to colour in this figure legend, the reader is referred to the Web version of this article.)

sensitivity and specificity can be established.

The results of this study show that miR378a-3p could be used as a biomarker that reflects pancreatic β-cell mass before the onset of diabetes, and that it may be possible to predict the onset of diabetes from an early stage and intervene, and it is hoped that this will contribute to the prevention of the onset of diabetes and an improved prognosis.

CRediT authorship contribution statement

Aisha Yokoi: Writing – original draft, Methodology, Investigation. **Shun-ichiro Asahara:** Writing – review & editing, Project administration, Conceptualization. **Hiroyuki Inoue:** Validation, Investigation. **Ayano Goto:** Investigation. **Masako Seike:** Validation, Investigation. **Nozomi Kido:** Investigation. **Hirotaka Suzuki:** Investigation. **Ayumi Kanno:** Investigation, Funding acquisition. **Maki Kimura-Koyanagi:** Visualization, Supervision. **Kenichi Uto:** Investigation. **Jun Saegusa:** Supervision. **Yoshiaki Kido:** Supervision. **Wataru Ogawa:** Supervision, Conceptualization.

Funding

This research was supported by a Grant-in-Aid for Creative Scientific Research from the Ministry of Education, Culture, Sports, Science and Technology (MEXT; 20K08860 to S.A.); a Grant-in-Aid for Creative Scientific Research from MEXT (22K08653 to A.K.); and a Grant-in-Aid for Creative Scientific Research from MEXT (21K08579 to Y.K.). The sponsor had no role in the study design, in the collection, analysis, or interpretation of data, in the writing of the report, or in the decision to submit the article for publication.

Declaration of competing interest

The authors declare that they have no known competing financial interests or personal relationships that could have appeared to influence the work reported in this paper.

Acknowledgments

We thank Y. Ogushi and K. Miyazaki for technical assistance.

Glossary

ELISA, enzyme-linked immunosorbent assay; EV, extracellular vesicle; KO, knockout; miRNA, microRNA; PBS, phosphate-buffered saline; PDK1, pyruvate dehydrogenase kinase 1; PDX1, pancreatic and duodenal homeobox 1; SEM, standard error of the mean; STZ, streptozotocin.

References

[1] GBD 2021 Diabetes Collaborators, Global, regional, and national burden of diabetes from 1990 to 2021, with projections of prevalence to 2050: a systematic analysis for the Global Burden of Disease Study 2021, Lancet 402 (2023) 203–234, https://doi.org/10.1016/s0140-6736(23)01301-6.

[2] C. Weyer, C. Bogardus, D.M. Mott, R.E. Pratley, The natural history of insulin secretory dysfunction and insulin resistance in the pathogenesis of type 2 diabetes mellitus, J. Clin. Invest. 104 (1999) 787–794, https://doi.org/10.1172/jci7231.

[3] S.I. Asahara, H. Inoue, H. Watanabe, Y. Kido, Roles of mTOR in the regulation of pancreatic β-cell mass and insulin secretion, Biomolecules 12 (2022) 614, https://doi.org/10.3390/biom12050614.

[4] G. Klöppel, M. Löhr, K. Habich, M. Oberholzer, P.U. Heitz, Islet pathology and the pathogenesis of type 1 and type 2 diabetes mellitus revisited, Surv. Synth. Pathol. Res. 4 (1985) 110–125, https://doi.org/10.1159/000156969.

[5] K. Kou, Y. Saisho, S. Satoh, T. Yamada, H. Itoh, Change in β-cell mass in Japanese nondiabetic obese individuals, J. Clin. Endocrinol. Metab. 98 (2013) 3724–3730, https://doi.org/10.1210/jc.2013-1373.

[6] M.W. Graner, Roles of extracellular vesicles in high-grade gliomas: tiny particles with outsized influence, Annu. Rev. Genom. Hum. Genet. 20 (2019) 331–357, https://doi.org/10.1146/annurev-genom-083118-015324.

[7] M. Feng, J. Zhao, L. Wang, J. Liu, Upregulated expression of serum exosomal microRNAs as diagnostic biomarkers of lung adenocarcinoma, Ann. Clin. Lab. Sci. 48 (2018) 712–718.

[8] A.M.L. Coenen-Stass, M.J. Pauwels, B. Hanson, C. Martin Perez, M. Conceição, M.J. A. Wood, I. Mäger, T.C. Roberts, Extracellular microRNAs exhibit sequence-dependent stability and cellular release kinetics, RNA Biol. 16 (109) 696–706. https://doi.org/10.1080/15476286.2019.1582956.

[9] X. Dong, D. Zheng, J. Nao, Circulating exosome microRNAs as diagnostic biomarkers of dementia, Front. Aging Neurosci. 12 (2020) 580199, https://doi.org/10.3389/fnagi.2020.580199.

[10] N. Hashimoto, Y. Kido, T. Uchida, S. Asahara, Y. Shigeyama, T. Matsuda, A. Takeda, D. Tsuchihashi, A. Nishizawa, W. Ogawa, Y. Fujimoto, H. Okamura, K. C. Arden, P.L. Herrera, T. Noda, M. Kasuga, Ablation of PDK1 in pancreatic beta cells induces diabetes as a result of loss of beta cell mass, Nat. Genet. 38 (2006) 589–593, https://doi.org/10.1038/ng1774.

[11] K. Uto, K. Ueda, T. Okano, K. Akashi, S. Takahashi, Y. Nakamachi, T. Imanishi, H. Awano, A. Morinobu, S. Kawano, J. Saegusa, Identification of plexin D1 on circulating extracellular vesicles as a potential biomarker of polymyositis and dermatomyositis, Rheumatology 61 (2022) 1669–1679, https://doi.org/10.1093/rheumatology/keab588.

[12] A.E. Butler, J. Janson, S. Bonner-Weir, R. Ritzel, R.A. Rizza, P.C. Butler, Beta-cell deficit and increased beta-cell apoptosis in humans with type 2 diabetes, Diabetes 52 (2003) 102–110, https://doi.org/10.2337/diabetes.52.1.102.
[13] S. Asahara, T. Matsuda, Y. Kido, M. Kasuga, Increased ribosomal biogenesis induces pancreatic beta cell failure in mice model of type 2 diabetes, Biochem. Biophys. Res. Commun. 381 (2009) 367–371, https://doi.org/10.1016/j.bbrc.2009.02.047.
[14] T. Matsuda, Y. Kido, T. Uchida, M. Kasuga, Reduced insulin signaling and endoplasmic reticulum stress act synergistically to deteriorate pancreatic beta cell function, Kobe J. Med. Sci. 54 (2008) E114–E121.
[15] A. Jones, K.M. Danielson, M.C. Benton, O. Ziegler, R. Shah, R.S. Stubbs, S. Das, D. Macartney-Coxson, miRNA signatures of insulin resistance in obesity, Obesity 25 (2017) 1734–1744, https://doi.org/10.1002/oby.21950.
[16] U. Can, M. Buyukinan, F.H. Yerlikaya, The investigation of circulating microRNAs associated with lipid metabolism in childhood obesity, Pediatr. Obes. 11 (2016) 228–234, https://doi.org/10.1111/ijpo.12050.
[17] E. Ferrannini, S. Camastra, A. Gastaldelli, A. Maria Sironi, A. Natali, E. Muscelli, G. Mingrone, A. Mari, Beta-cell function in obesity: effects of weight loss, Diabetes 53 (2004) S26–S33, https://doi.org/10.2337/diabetes.53.suppl_3.s26.
[18] N. Huang, J. Wang, W. Xie, Q. Lyu, J. Wu, J. He, W. Qiu, N. Xu, Y. Zhang, MiR-378a-3p enhances adipogenesis by targeting mitogen-activated protein kinase 1, Biochem. Biophys. Res. Commun. 457 (2015) 37–42, https://doi.org/10.1016/j.bbrc.2014.12.055.
[19] W. Liu, H. Cao, C. Ye, C. Chang, M. Lu, Y. Jing, D. Zhang, X. Yao, Z. Duan, H. Xia, Y. C. Wang, J. Jiang, M.F. Liu, J. Yan, H. Ying, Hepatic miR-378 targets p110α and controls glucose and lipid homeostasis by modulating hepatic insulin signalling, Nat. Commun. 5 (2014) 5684, https://doi.org/10.1038/ncomms6684.
[20] M. Carrer, N. Liu, C.E. Grueter, A.H. Williams, M.I. Frisard, M.W. Hulver, R. Bassel-Duby, E.N. Olson, Control of mitochondrial metabolism and systemic energy homeostasis by microRNAs 378 and 378, Proc. Natl. Acad. Sci. U.S.A. 109 (2012) 15330–15335, https://doi.org/10.1073/pnas.1207605109.
[21] I.F. Machado, J.S. Teodoro, C.M. Palmeira, A.P. Rolo, miR-378a: a new emerging microRNA in metabolism, Cell. Mol. Life Sci. 77 (2020) 1947–1958, https://doi.org/10.1007/s00018-019-03375-z.
[22] F. Syed, D. Singhal, K. Raedschelders, P. Krishnan, R.N. Bone, M.R. McLaughlin, J. E. Van Eyk, R.G. Mirmira, M.L. Yang, M.J. Mamula, H. Wu, X. Liu, C. Evans-Molina, A discovery-based proteomics approach identifies protein disulphide isomerase (PDIA1) as a biomarker of β cell stress in type 1 diabetes, EBioMedicine 87 (2023) 104379, https://doi.org/10.1016/j.ebiom.2022.104379.
[23] M.L. Yang, S. Horstman, R. Gee, P. Guyer, T.T. Lam, J. Kanyo, A.L. Perdigoto, C. Speake, C.J. Greenbaum, A. Callebaut, L. Overbergh, R.G. Kibbey, K.C. Herold, E.A. James, M.J. Mamula, Citrullination of glucokinase is linked to autoimmune diabetes, Nat. Commun. 13 (2022) 1870, https://doi.org/10.1038/s41467-022-29512-0.
[24] K. Khoshnevisan, H. Baharifar, F. Torabi, M. Sadeghi Afjeh, H. Maleki, E. Honarvarfard, H. Mohammadi, S.M. Sajjadi-Jazi, S. Mahmoudi-Kohan, F. Faridbod, B. Larijani, F. Saadat, R. Faridi Majidi, M.R. Khorramizadeh, Serotonin level as a potent diabetes biomarker based on electrochemical sensing: a new approach in a zebra fish model, Anal. Bioanal. Chem. 413 (2021) 1615–1627, https://doi.org/10.1007/s00216-020-03122-5.